Vertical Dynamics Description and its Control in the Presence of Nonlinear Friction

Ferch, Tobias; Mercorelli, Paolo

Vertical Dynamics description and its Control

in the Presence of Nonlinear Friction

TOBIAS FERCH and PAOLO MERCORELLI
Institute of Product and Process Innovation
Leuphana University Lueneburg
Universitätsallee 1, 21335 Lueneburg, Germany
mercorelli@uni.leuphana.de

Abstract: - This paper deals with a control of a vertical dynamics in the presence of nonlinear friction in a robotic mechanism. The control structure, which is taken into consideration, is the Sliding Mode Control (SMC). Using this control technique, it is possible to show the asymptotical stability of the trajectory to be tracked. Simulation results show the effectiveness of the proposed control technique.

Key-Words: - Mechanical systems - Mechanical friction – Displacement - SMC – Applications - Simulations

1 Introduction

This paper extends the results already obtained in [1] with particular emphasis on some aspects the friction phenomenon including more simulation cases. In the course of Industry 4.0, the use of robotic systems in industrial manufacturing is increasingly playing an essential role. Moreover, the use of industrial robots is based on the guaranteed uniformity and precision that such a system offers. In this case, the robot can do different tasks. For example, it can be used independently in series production or supportive and it can serve the person as a helper at work. The articulated robots used in industry are usually constructed as an open kinematic chain. In this design, each arm part of the robot is connected via a joint to the following arm part. The last arm part of the chain is called the effector: this is the part of the robot that interacts with the environment. Tasks in which the effector enters into mechanical contact with objects within its environment are normal. Therefore, the contact force plays an essential role in the control of such systems. Since industrial robots are mainly operated position-controlled, the control of the contact force and the position control are related to each other. In order to move an object from its starting position to the target position, individual or cooperating robots are used in industrial production, these have as effector predominantly a variant of a gripper. The joint gripping of an object offers the advantage of load sharing, in contrast, this also leads to the closing of a kinematic chain between the two robots. As a result of this connection, the two robots mutually influence each other during their movement, as a result of which undesired changes in the relative robot position can occur, resulting in resultant forces in the workpiece. To avoid this problem, this work deals with the clawless position control of an object. In this case, an articulated robot is considered, which regulates the vertical position of an object solely by the applied contact pressure. In this case, the actual position of the object centre point should follow the desired set point position in a uniform movement. The control was realized with a Sliding Mode Control (SMC), this method offers the necessary flexibility and robustness to enable a valid analysis, in particular in an application field, [2], [3], [4]. The paper is organized as follows. In Section 2 some physical basic knowledge are considered. Section 3 considers the construction of the model using differential equations. Section 4 presents the obtained results. Discussion, conclusion and outlook close the paper.

2 Background

For simplification, the object is pressed against a rigid surface by the robot arm (Fig.1). One possible type of control of an articulated robot is the path control. In this motion control, from given velocity and acceleration, orbits are calculated with respect to the effector in the world coordinate system. The

path control enables a movement on a straight line with the aid of linear interpolation. Here, the centre of the effector (also called TCP = Tool Centre Point) serves as a reference point for the movement on the linear path. This type of motion allows viewing robot dynamics in the horizontal plane, starting from the centre of the effector. The contact forces, due to Coulomb friction, provide a nonlinearity of dynamics. One of the core tasks is the modelling of the dynamics in order to be able to simulate system behaviour close to reality..
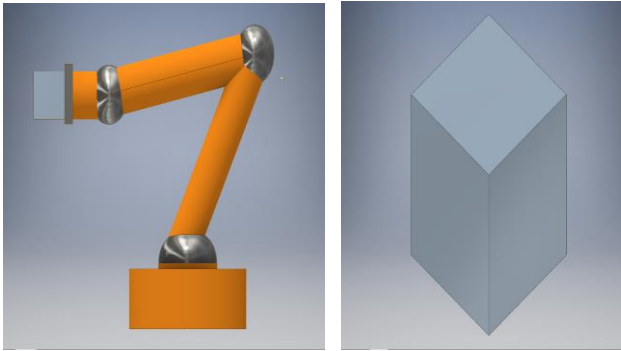

Figure 1: Schematic representation of robotic arm and object

The field of control engineering makes it possible to describe the behaviour of dynamic systems based on their signals and the transformations of these signals. Signals are time-variable quantities which are processed and transmitted by a dynamic system. Because of this, differential equations typically form the basis of models. These contain signals and their time derivatives, as well as system-dependent physical parameters. The established differential equations make it possible to determine the time course of the output variable as a function of the input variable. In the process, the effects of the control parameters and the relationships of the control loop are recorded, which enables targeted intervention in the system. In order to arrive at the desired model via the relationships of the control loop, it is necessary to deduce the physical character of the dynamic processes. Here, temporal processes are described by time functions and the relationships between the processes as functional dependencies between these time functions. The temporally variable description variables of physical phenomena are decisive, as they reflect the dynamic behaviour of the system under consideration. In the following the physical basics for the derivation of the required differential equations are presented.

2.1   Physical basics

Coulomb's law of friction deals with dry friction between solid bodies and, due to its manifold applicability, it is an extremely complicated physical phenomenon. As a result of force-forced contact between two material surfaces, normal systems produce both normal forces and frictional forces. Two causes of microscopic nature are mainly responsible for the development of friction forces. Molecules tend to fall below of a minimum distance under pressure or heating to form molecular bonds. The second cause is roughness of the contact surfaces, this leads locally to different directions of the common normal surface, this tends to follow a rotation of the common normal surface in the direction of preventing any movement.
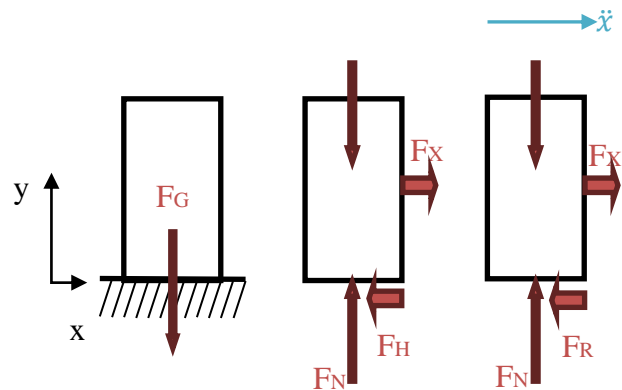

Figure 1: Frictional movement on a horizontal plane

In Fig. 1, a body is pressed by its weight F_G on a horizontal rough surface. The force of gravity counteracts an equally large normal force F_N acting perpendicularly to the surface:

$$F_G = F_N = mg \tag{1}$$

If the body is moved by a force F_x at constant speed $\dot{x}(t)$, the frictional force must be overcome. This counteracts the sense of direction of the movement tangentially in the contact surface. If the acting force F_x is not sufficient to overcome the resistance force generated by the friction, this form of resistance is called the static friction force F_H. With

the help of the free body image and the equilibrium condition, the following relations result:

$$\uparrow:\ F_N = F_G,\quad \rightarrow:\ F_H = F_x. \tag{2}$$

Charles Augustine de Coulomb has shown by experiments that as long as a horizontal force F_x remains below a limit F_0, then $F_H(t) = F_x(t)$, where $F_H(t)$ represents the friction force which can be considered in a possible movement. If the force reaches this limit, $F_H(t)$ assumes its maximum value F_{H0}. Furthermore, Coulomb's experiments showed that the normal force and the limit F_{H0} are proportional in a first approximation and it results as follows:

$$F_{H0} = \mu_0 F_N(t). \tag{3}$$

The proportionality factor μ_0 is called the coefficient of adhesion, which depends on the materials of the surfaces. If the limit is exceeded, the body moves on a rough surface, while the sliding friction force F_R occurs as an impressed force. This is opposite to the direction of movement and is therefore also a resisting force. Since the body moves in this scenario, the basic equation of kinetics of the mechanism results as follows:

$$m\ddot{x}(t) = F_x(t) - F_R(t). \tag{4}$$

Coulomb's experiments have shown that frictional force $F_R(t)$ is also proportional to normal force $F_N(t)$ and simultaneously independent of velocity. This results in the following basic physical law:

$$F_R(t) = \mu F_N(t). \tag{5}$$

Here, the proportionality factor μ is called the friction coefficient. The two coefficients are always less than one, hence $F_H(t)$ and $F_R(t)$ are always fractions of the normal force $F_N(t)$. The dimension of the factors is a material constant and is determined experimentally between two surfaces. The foundations of tribology listed here revealed the following findings applied to the vertical system. Since this is a dynamic scheme, these findings were determined in a time-dependent manner. The weight force $F_G(t)$, which previously pressed the body to the plane, now acts as a driving force for the movement in the y-direction. The body is brought into its equilibrium situation by the contact force $F_{Rx}(t)$, acting through the robot. The free-body image of this system provides information about the position of the normal force and the static friction force:

$$\leftarrow:\ F_N(t) = F_{Rx}(t),\quad \downarrow:\ F_H(t) = F_G(t). \tag{6}$$

According to Coulomb's laws, the limit is approximately for the static friction force $F_H(t)$:

$$F_{H0}(t) = \mu_0 F_N(t) = \mu_0 F_{Rx}(t). \tag{7}$$

The static friction force is thus directly dependent on the acting contact force $F_{Rx}(t)$ of the robot. In the equilibrium position of the system the following relations hold:

$$F_H(t) = \mu_H F_{Rx}(t), \tag{8}$$

$$F_H(t) > F_G(t). \tag{9}$$

Accordingly, if the robot exerts a contact force $F_{Rx}(t)$ which, in conjunction with the static friction coefficient μ_H, is greater than the weight of the body, it is prevented from moving. If this is not the case, the body moves in the positive y-direction defined here. From the basic equation of the kinetics follows:

$$m\ddot{y}(t) = F_G(t) - F_H(t) = mg - k_H F_{Rx}(t), \quad \text{with} \tag{10}$$
static friction coefficient k_H

$$m\ddot{y}(t) = F_G(t) - F_R(t) = mg - k_R F_{Rx}(t) \quad \text{with} \tag{11}$$
coefficient of friction k_R.

2.2 The viscoelasticity

The horizontally acting force of the robot $F_{Rx}(t)$ causes deformation of the body, any deformation or return of a body is time-dependent. If the load is released, a time-dependent complete recovery of the material is called viscoelasticity. This behaviour can

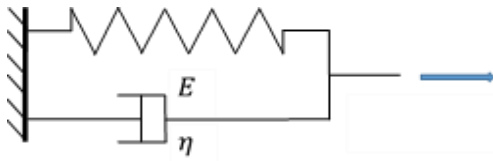be simplified with the help of a Kelvin-Voigt element (Fig. 2), see [5].

Figure 2: Parallel connection spring and damper element

To determine the behaviour of viscoelastic materials, characteristic material functions are experimentally developed. Viscoelastic fabrics have both elastic and viscous properties.
The viscoelastic factors are cumulated in this constant in the constant k_c. From the factor of viscoelasticity and the movement of the centre of mass in the x-direction, this relationship results for the viscoelastic resistance $F_c(t)$:

$$F_c(t) = k_c x_m(t). \tag{12}$$

2.3 The flow resistance

The body of the object is flowed around by the fluid air, the body prevents the fluid particles from flowing straight along the streamlines. As a result, the fluid is deflected and flows past the body. Now, as the body moves through the fluid, it creates a resistive force that counteracts the movement of the body. In contrast to the Coulomb friction, the resistance increases with increasing speed. Other influencing factors are the shape of the body and the fluid properties of the fluid. At low speeds, there is approximately a proportionality between speed and drag. At higher speeds, the force increases in proportion to the square of the speed. Assuming gravity to be constant and accelerating the object down from rest, the equation for flow resistance is given:

$$F_L(t) = b|v(t)|^n \tag{13}$$

with b und n being constants.

This general formula of flow resistance begins to become inaccurate even at speeds of a few meters per second. With the help of the Bernoulli equation, an equation can be derived which has a much higher accuracy. Assuming that the body around which it flows lowers the velocity of the fluid directly behind the body to zero, the pressure difference between

the faces perpendicular to the flow direction results: Figures and Tables should be numbered as follows:

$$\Delta p = \frac{1}{2}\rho v(t)^2. \tag{14}$$

Since $p = F/A$, the drag force can be calculated based on the dynamic pressure. From this assumption, the general formula for the Newtonian resistance force follows:

$$F_L(t) = \frac{1}{2}cA\rho v(t)^2. \tag{15}$$

The constant c is the coefficient of resistance, this refers to the entire shape of the body and is determined experimentally. Since the shape of the body and the material properties can be neglected in the course of this research work, the following forms can be derived from the laws listed here:

$$F_L(t) = k_L v(t). \tag{16}$$

The factor k_L is a constant which includes all system-specific factors and serves as a substitute for them. Thus, the flow resistance is only in proportion to this factor and the respective speed. From this form results for the dynamics in the x- and y-direction:

$$F_{Ly}(t) = k_{Ly}\dot{y}(t) \qquad \text{and}$$
$$F_{Lx}(t) = k_{Lx}\dot{x}(t). \tag{17}$$

3 Modelling

The physical phenomena and laws listed in the previous section allow to set up the necessary differential equations, which serve as a basis for the subsequent modelling. When setting up a differential equation, basically four steps can be used. In the first step, the system is broken down into its individual components. Subsequently, the physical laws are formulated, which describe the behaviour of the components. This step was already done in the previous section. In the third step, the coupling relationships between the components are established, and in the final, fourth step, the determined equations are then combined to form a differential equation. Since the target is the position control of the object in the vertical plane, three differential equations are needed in total.

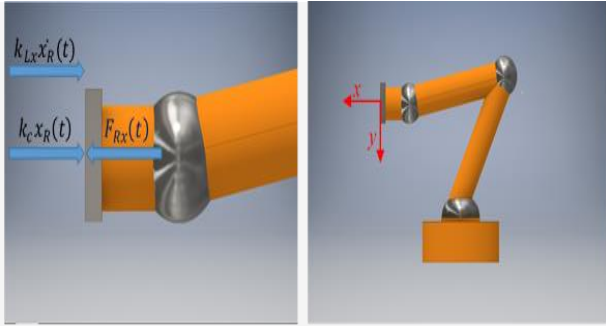## 3.1 DGL I horizontal dynamics of the robot

Figure 3: Free cut robot arm

The cut-out in Fig. 3 provides the position of the forces on the robot arm:

$$\leftarrow : 0 = F_{Rx}(t) - k_c x_R(t) - k_{Lx}\dot{x}_R(t), \qquad (18)$$

with $x_R(t)$ as the movement of the robot in the positive x-direction and $\dot{x}_R(t)$ as the associated movement speed. The origin of the coordinate system lies at the centre of the tool tip, as shown in the figure above. The resistance of the air and the resistance of the viscoelasticity counteract pressure of the robot. In conjunction with the basic equation of kinetics, the following differential equation results:

$$m_R \ddot{x}_R(t) = \sum F_x(t), \qquad (19)$$

$$m_R \ddot{x}_R(t) = F_{Rx}(t) - k_c x_R(t) - k_{Lx}\dot{x}_R(t). \qquad (20)$$

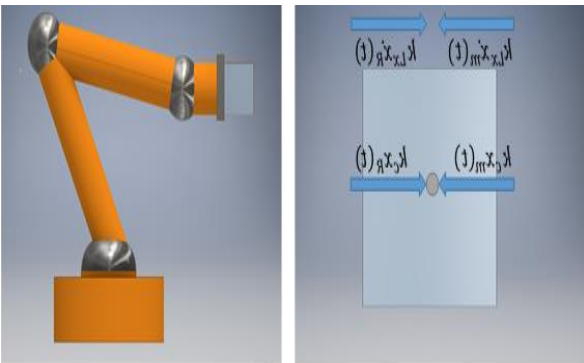## 3.2 DGL II horizontal dynamics of the object

Figure 4: Free cut object horizontal

The free-body image in Fig. 4 shows the position of the forces between the robot arm and the object:

$$\leftarrow : 0 = k_c x_R(t) - k_c x_m(t) + k_{Lx}\dot{x}_R(t) - k_{Lx}\dot{x}_m(t)$$

$$0 = k_c(x_R(t) - x_m(t)) + k_{Lx}(\dot{x}_R(t) \qquad (21)$$

$$-\dot{x}_m(t)),$$

with $x_m(t)$ as movement of the mass in positive x-direction and $\dot{x}_m(t)$ as associated movement speed. These assumptions are to be considered in the context of the DGL. The movement of the robot arm causes a deformation of the object and thus moves the centre of gravity of the body. Under these conditions the following dynamic behaviour results:

$$m\ddot{x}_m(t) = \sum F_x(t) \qquad (22)$$

$$m\ddot{x}_m(t) = k_c(x_R(t) - x_m(t))$$

$$+k_{Lx}(\dot{x}_R(t) - \dot{x}_m(t)). \qquad (23)$$

As a result, the horizontal movement of the centre of mass counteracts the flow resistance of the air and its own viscoelastic properties. These forces are directly related to the movement of the robot arm.

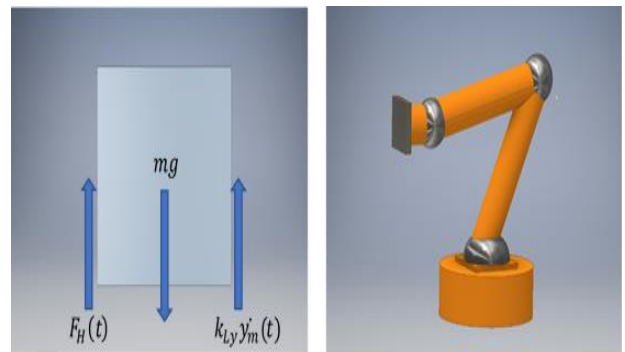## 3.3 DGL III vertical dynamics of the object

Figure 5: Free-cutting object vertical

The free-body image in Fig. 5 provides the forces acting vertically on the body:

$$\downarrow : 0 = mg - F_H(t) - k_{Ly}\dot{y}_m(t) \text{ at rest} \qquad (24)$$

$$\downarrow : 0 = mg - F_R(t) - k_{Ly}\dot{y}_m(t) \text{ in motion.} \qquad (25)$$

If the weight force $F_G(t)$ is below the limit value of the adhesive condition, the body remains in its equilibrium position. If the limit of static friction is exceeded, the body starts to move. This movement counteracts the resistance of Coulomb friction and slows down the body. Furthermore, the flow resistance of the air counteracts the movement. Information about the dynamic behaviour provides again the basic equation of the kinetics:

$$m\ddot{y}_m(t) = \sum F_y(t) \qquad (26)$$

$$m\ddot{y}_m(t) = mg - F_H(t) - k_{Ly}\dot{y}_m(t) \qquad (27)$$

$$m\ddot{y}_m(t) = mg - F_R(t) - k_{Ly}\dot{y}_m(t). \qquad (28)$$

4 The Sliding Mode Control: Background and its Applications

SMC is one of the most important control strategies in the field of nonlinear control, [6], [7], [8], [9] and [10]. The dynamics of the overall system modelled in this way do not yet offer any possibility of regulating the position of the object based on a desired setpoint position. Only the parameter $F_{Rx}(t)$ determines by the friction law whether the body starts to move or the rest position is maintained. The aim now is to define the contact force $F_{Rx}(t)$ so that it can be regulated as a function of the actual and desired position. In formulating any practical regulatory task, there will always be a certain discrepancy between reality and the mathematical model. These discrepancies are based on unknown external interfering signals, system parameters and non-modelled dynamics. The challenge is to develop controller laws that provide

the desired performance in the presence of these disturbing influences. Therefore, there is an increasing interest to develop such robust control methods. One of these robust methods is the so-called Sliding Mode Control (SMR), which belongs to the field of variable structured control. Variable Structured Control (VSR) covers (2) wide range of different system types, including nonlinear systems, multi-input multi-output systems, large scale systems, and infinite dimensional systems. The main feature of the VSR is the invariance over certain limited noise and parameter variations. Slip state controllers switch between two control laws depending on the state vector. The basic principles of SMR can be explained by considering a simple linear controlled system.

$$\dot{x}_1 = x_2 \qquad x_1(0) = x_{10} \qquad (29)$$

$$\dot{x}_2 = u + f(x_1, x_2, t) \qquad x_2(0) = x_{20.} \qquad (30)$$

With u as the input and $f(x_1, x_2, t)$ as the term containing any system resistive forces. Basically, the task of the input variable $u = u(x_1, x_2)$ is to control the state variables of the system to zero:

$$\lim_{t \to \infty} x_1, x_2 = 0. \qquad (31)$$

The goal of asymptotic convergence in the presence of the unknown limits of the resistance forces $f(x_1, x_2, t)$ is a demanding regulatory task. For example, the following linear feedback control law would provide asymptotic stability of origin, just for the case $f(x_1, x_2, t) = 0$.

$$u = -k_1 x_1 - k_2 x_2, \qquad k_1 > 0, \ k_2 > 0. \qquad (32)$$

To solve this problem, the SMR uses a compensation dynamics $s(t)$, the so-called switching hyperplane or sliding surface. This switching function is defined as follows:

$$s(t) = C_s x(t). \qquad (33)$$

The vector C_s contains coefficients which describe the switching level as a function of the state vector $x(t)$. The value of s specifies the distance of a point to the switching plane, hence $s = 0$ means that the

point lies on the switching hyperplane. Defining the switching level as follows:

$$s = c_{s1}x_1 + C_{s2}x_2 + \cdots + c_{sn-1}x_{n-1} + x_n = 0$$

(34)

$$x_n = -c_{s1}x_{s1} - c_{s2}x_2 - \cdots - c_{sn-1}x_{n-1} \qquad (35)$$

$$\dot{x}_n = -c_{s1}x_2 - c_{s2}x_3 - \cdots - c_{sn-2}x_{n-1}$$

$$+ \sum_{i=1}^{n-1} c_{sn-1}c_{si}x_i \qquad (36)$$

the entire dynamics of the system are governed by the parameters of the switching hyperplane:

$$\dot{x}_n = -c_{s1}x_2 - c_{s2}x_3 - \cdots - c_{sn-2}x_{n-1} + \sum_{i=1}^{n-1} c_{sn-1}c_{si}x_i \qquad (37)$$

$$\dot{x}_i = x_{i+1}, \qquad i = 1, 2, \dots, n-1. \qquad (38)$$

As a result, the system dynamics have independence from the system parameters and only depend on the parameter C_s of the switching level. This is proof of the robustness of the SMR against parameter fluctuations. A general basic formula for determining the switching function can have the following form:

$$s(t) = \left(\frac{d}{dt} + k_s\right)^{n-1} \Delta x(t) \qquad (39)$$

with

$$\Delta x(t) = x(t) - x_d(t) =$$

$$\left[\Delta x(t), \Delta \dot{x}(t), \dots, \Delta x(t)^{(n-1)}\right]^T \text{ and } k_s > 0. \qquad (40)$$

In the case of a position control, $x(t)$ corresponds to the actual value of the position which follows the setpoint value $x_d(t)$ in a finite time. To make this possible, the initial condition $x_d(0) = x(0)$ must be fulfilled. To initialize a slip state, another aspect is essential besides stability. This includes the reachability of the switching level for all trajectories of the state space. To ensure this accessibility, a necessary condition is that the trajectories of the control loop on both sides converge to the switching level. This can be expressed by the following conditions for the switching function:

$$\dot{s}(t) < 0 \qquad \text{for} \qquad s(t) > 0 \qquad (41)$$

$$\dot{s}(t) > 0 \qquad \text{for} \qquad s(t) < 0. \qquad (42)$$

These two conditions can be summarized in the reachability condition:

$$s(t)\dot{s}(t) < 0. \qquad (43)$$

The following example illustrates, however, that the reachability condition is not sufficient to establish the slip state.

$$\dot{s}(t) = -s(t) \qquad (44)$$

$$s(t)\dot{s}(t) = -s(t)^2, \ \forall s(t) \neq 0. \qquad (45)$$

The solution for this is given by:

$$s(t) = e^{-t}s(0). \qquad (46)$$

This has the consequence that $s(t) = 0$ is only given for $t \to \infty$, when approaching the switching level, it takes infinite time to reach them. A common approach for solving this problem is that of Gao and Hung. Here, the decrease of the switching function along the trajectories is specified.

$$\dot{s}(t) = -Bsgn\big(s(t)\big) - \lambda s(t) \tag{47}$$

with B and λ as strictly positive constants, this makes it possible to fulfil the reachability condition:

$$s(t)\dot{s}(t) = -B|s(t)| - \lambda s(t)^2 < 0. \tag{48}$$

The parameters B and λ are freely selectable parameters which make it possible to influence the rate of change of the switching function constantly and proportionally.

4.1 Lyapunov Approach: Background

One of the prerequisites for the induction of a sliding mode control is the verification of the system stability, with respect to the switching hyperplane. One method which lends itself to the general stability analysis of nonlinear systems is the stability theory of A.M. Lyapunov. This procedure makes it possible in principle to examine all dynamic systems for their stability. A variant to prove the stability according to the Lyapunov stability theory is to show the dependence of the derivative $\dot{V}(t)$ of the suitable Lyapunov function $V(t)$ on the input u. In this case, it should be demonstrated that for every meaningfully chosen value of u, the derivative

$$\dot{V}(t) < 0. \tag{49}$$

This is because an equilibrium state is considered stable if it is possible to find a Lyapunov function of the system state which has its minimum in the rest position of the system and whose value decreases along each trajectory of the system. This behavior allows to guarantee stability without a solution to the differential equation of the system. From these conditions, two basic steps can be formulated. The Lyapunov function and its derivative should be chosen so that the distance to the sliding surface and its rate of change have inverted signs. Furthermore, a controller should be chosen that meets the selected stability criteria. In addition, the selection should aim to find a Lyapunov function that has the greatest possible simplicity.

Looking at the following simple differential equation, it is possible to establish the stability criteria according to Lyapunov.

$$\dot{x} = f(x) \qquad\qquad x_R = 0. \tag{50}$$

For every initial value from an environment $U_1(0)$ of origin, the equation has a continuous and unique solution. Now there exists a function $V(t)$ with the following properties:

$$V(0) = 0. \tag{51}$$

It is continuous in the environment and has continuous partial derivatives. Furthermore, with the exception of $t = 0$, it fulfils the following conditions:

$$V(t) > 0 \tag{52}$$

$$\dot{V}(t) \le 0, \tag{53}$$

then, the system results to be stable.

$$\dot{V}(t) < 0, \tag{54}$$

then, the system results to be asymptotically stable.

So, the rest position is stable or asymptotically stable in the sense of Lyapunov. If the function $V(t)$ satisfies these three conditions, the stability is proven. It should be noted that the physical meaning of the function itself is not critical. The direct method of Lyapunov therefore returns the problem of stability analysis to a functional Lyapunov function. There is no systematic method for formulating the Lyapunov function which certainly generates the optimal function for a nonlinear system.

4.2 Application of the Sliding Mode Control

The switching function of the dynamics results from the following general basic equation:

$$s(t) = \left(\frac{d}{dt} + k_s\right)^{n-1} \Delta x(t) \tag{55}$$

with

$$\Delta x(t) = x(t) - x_d(t). \qquad (56)$$

The goal is to control the position of the body in a vertical plane. For these dynamics a differential equation of the second order exists, from which it follows with $n = 2$:

$$s(t) = (\frac{d}{dt} + k_s)\Delta y(t). \qquad (57)$$

$$s(t) = \dot{y}_m(t) - \dot{y}_{md}(t) \qquad (58)$$

$$+ k_s(y_m(t) - y_{md}(t)).$$

The following Lyapunov function is suitable for this switching function, with the condition

$$V(0) = 0. \qquad (59)$$

Considering

$$V(s(t)) = \frac{1}{2}s^2(t). \qquad (60)$$

This function satisfies the condition $V(t) > 0$ of Lyapunov, the differentiation of this function leads to:

$$\dot{V}(s(t)) = s(t)\dot{s}(t). \qquad (61)$$

This corresponds to the desired shape. The insertion of the sliding surface leads to:

$$\dot{V}(t) = s(t)[\ddot{y}_m(t) - \ddot{y}_{md}(t) + ks(\dot{y}_m(t) \qquad (62)$$

$$- \dot{y}_{md}(t))].$$

Subsequent insertion of the equation (28) for $\ddot{y}_m(t)$:

$$\dot{V}(t) = s(t)\left[g - \frac{F_H(t) - k_{Ly}\dot{y}_m(t)}{m} \qquad (63)\right.$$

$$- \ddot{y}_{md}(t) + ks(\dot{y}_m(t)$$

$$\left. - \dot{y}_{md}(t))\right]$$

and the substitution of $F_H(t)$ leads to:

$$0 = g - \frac{F_H(t) - k_{Ly}\dot{y}_m(t)}{m} - \ddot{y}_{md}(t) + ks(\dot{y}_m(t)-$$

$$\dot{y}_{md}(t)) \qquad (64)$$

$$F_H(t) = -k_{Ly}\dot{y}_m(t) + m[-\ddot{y}_{md}(t) + \qquad (65)$$

$$ks(\dot{y}_m(t) - \dot{y}_{md}(t)) + g].$$

Taking into account the following relation:

$$F_H(t) = -k_{Ly}\dot{y}_m(t) + m[-\ddot{y}_{md}(t) +$$

$$ks(\dot{y}_m(t) - \dot{y}_{md}(t)) + g] + m\lambda s(t) +$$

$$mBsgn(s(t)). \qquad (66)$$

Subsequent insertion of the substitution term in $\dot{V}(t)$:

$$\dot{V}(t) = s(t)[-\lambda s(t) - Bsign(s(t))]. \qquad (67)$$

With the condition $\lambda, B > 0$ it follows:

$$\dot{V}(t) = -\lambda s(t)^2 - B|s(t)| < 0. \qquad (68)$$

The stability condition of Lyapunov is thus fulfilled and also the asymptotic stability of the rest position. The relationship between the contact force $F_{Rx}(t)$ and the static friction force $F_{Rx}(t)$ is given by:

$$F_H(t) = (F_{Rx}(t) - k_c(x_m(t) - x_R(t))k_H. \qquad (69)$$

The required contact force to produce the stiction state is thus defined by:

$$F_{Rx}(t) = \frac{F_H(t)}{k_H} + k_c(x_m(t) - x_R(t)). \qquad (70)$$

Inserting the switching function leads to:

$$
\begin{aligned}
&F_{Rx}(t) \\
&= k_c(x_m(t) - x_R(t)) \\
&+ \frac{-k_{Ly}\dot{y}_m(t) + m[-\ddot{y}_{md}(t) + ks(\dot{y}_m(t) - \dot{y}_{md}(t))]}{k_H}
\end{aligned}
$$

$$+ m\left[\frac{+g + \lambda s(t) + B sgn(s(t))]}{k_H}\right]. \qquad (71)$$

Thus, a SMC was derived taking into account the stability theory of Lyapunov and the reachability condition of the switching hyperplane. With the help of this it is now possible to control the actual position of the object solely on the basis of the desired position.

5 Simulations

It is used to vary parameters in the course of the investigation in order to analyse the control and in order to show how the disturbance can influence the behaviour of the controlled system.
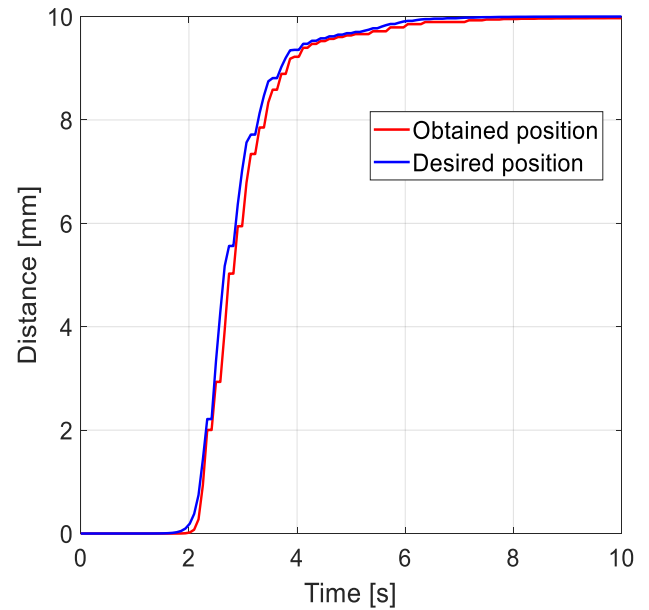

Figure 6: Target (blue line) and actual position (red line)

• All graphs of the actual position are marked with a red colour

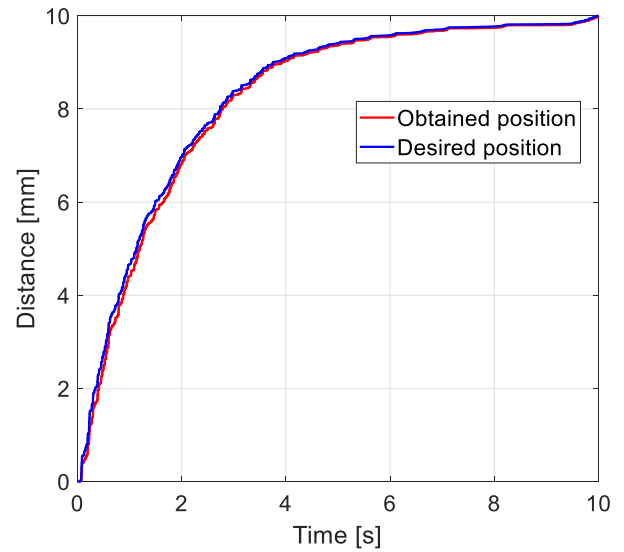• All graphs of the nominal position are marked with the blue colour.

The function graphs in Fig. 6 show a possible behaviour between the set point and the actual position. The simulation time was set at ten seconds and the desired movement of the body was defined to 10 mm. The desired position is asymptotic in the approach to the target position. However, it is also clear that the entire sequence of movements is not a uniform movement, in addition to the target position is not fully achieved. With the parameters λ and B, the SMC has tuning parameters, which offer the possibility of optimizing the SMC and thus smoothing the present motion sequence. A significant change in the system behaviour in the range λ, $B <1$, could not be determined.

Figure 7: Simulation for λ = 100 and B=1
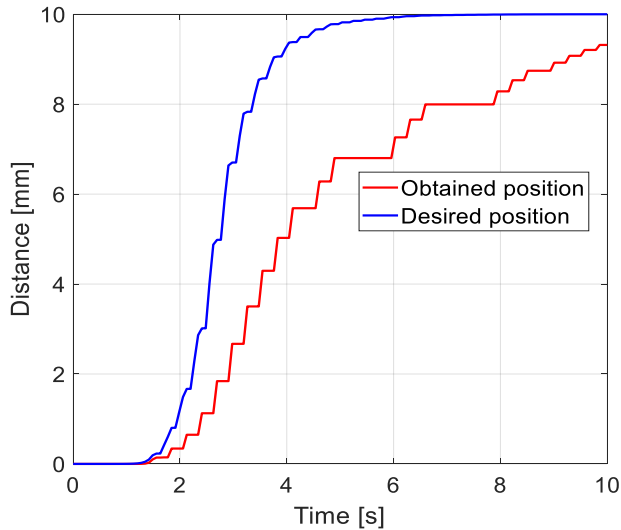

Figure 8: Simulation for λ = 1000 and B=1

It was therefore necessary to investigate how the dynamics change when the parameters in the range λ and *B*> 1 are increased. First, the behaviour of the function graph at a constant value of *B* = 1 and the change of λ is investigated. Setting λ = 100 produces the result graphed in Fig. 7. The achievement of the desired position is thereby not possible. However, some increase in the switching frequency during the sliding phase of the switching function which is noticeable. Of interest is now the behaviour of the function with further increase of the factor. The function graph in Fig. 8 corresponds to the behaviour at λ = 1000. The actual position follows here approximately the desired position on the entire route. The movement provides a much more stable pattern along the entire route. When enlarging the graphs, however, it became clear that even here the target position is not completely reached. There is a small difference between the actual value and the set point value every time t.

$$\Delta y(t) = y_m(t) - y_{md}(t) > 0. \qquad (72)$$

By simply tuning the parameter λ, the sliding surface cannot be met.

It was therefore necessary to investigate whether and to what degree the parameter *B* can improve the system behaviour in terms of control. As in the previous analysis, the value of a parameter is kept constant, here λ = 1. The function graph in Fig. 9 shows the system behaviour with a parameterization of *B* = 100.
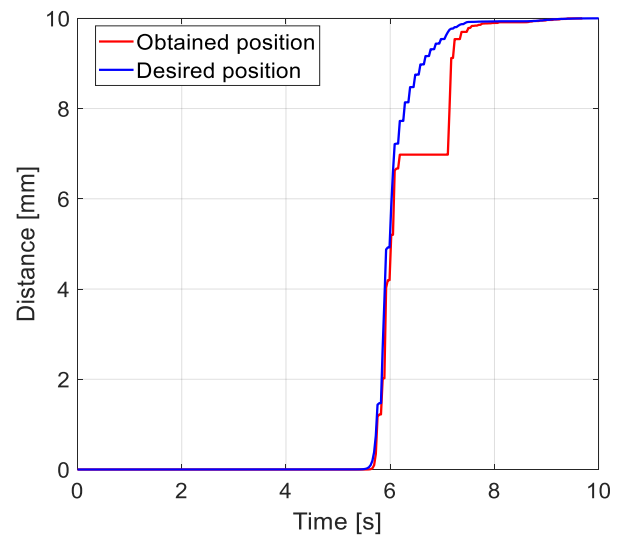
Figure 9: Simulation for λ = 1 and B = 100

In contrast to the λ parameter, the *B* parameter does not seem to exert a significant influence on the switching frequency of the graph. However, it is clear that the actual position reaches the target position asymptotically. After reaching the desired position $\Delta y(t) = y_m(t) - y_{md}(t) = 0$, the dynamics is maintained at the switching hyperplane.
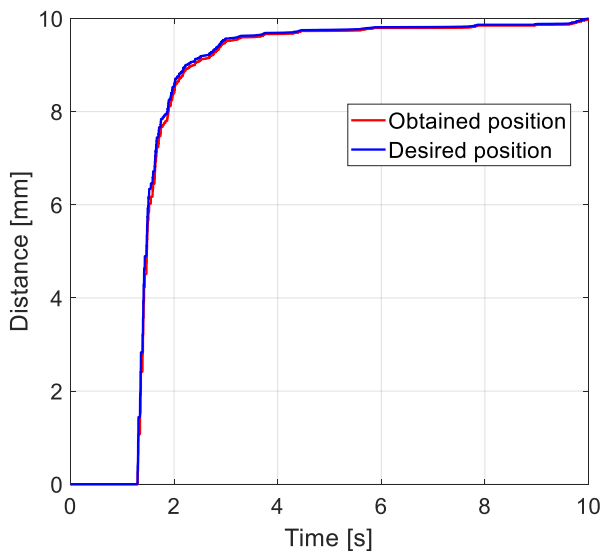
Figure 10: Simulation for λ = 1 and B = 1000

Further increasing the parameter $B = 1000$ gave the result of Fig. 10. The feature now provides a significant improvement in stability during the sliding phase. It follows that during this phase the parameter has an influence on the rate of change of the switching function.
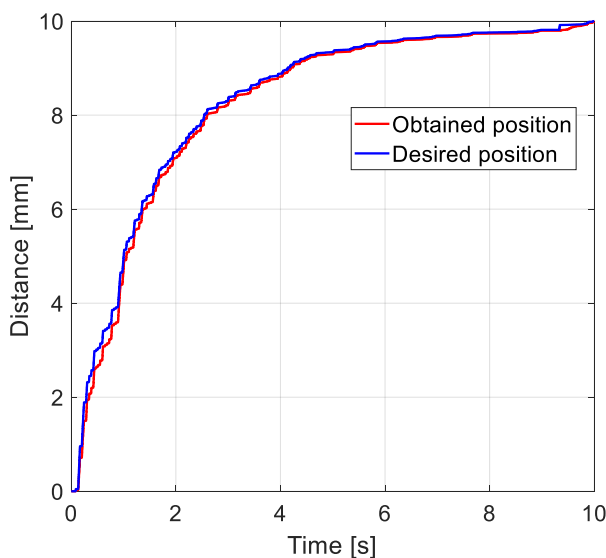

Figure 11: Simulation for λ = 500, B = 100

It is thus proven that the connection of the two parameters can unmistakably contribute to achieving the desired performance. The result of the connection and tuning of the two parameters is shown in Fig. 11. This function graph now offers asymptotic stability during the sliding phase in the

direction of the desired position. In addition, the rate of change is designed so that the actual position follows the desired position during the sliding phase in an approximately uniform movement.

$$s(t)\dot{s}(t) = -B|s(t)| - \lambda s(t)^2 < 0. \qquad (79)$$

The values $\lambda = 500$ and $B = 100$ were determined experimentally and a further optimization of the parameterization is not excluded.

5.1 Disturbance behaviour

The robustness of the SMR, in contrast to limited external disturbances, now had to be proven as well. One potential source of interference could be bumped on the surface of the object. The simulation of this case was realized with the help of the Sine Wave function block. The sine wave block generates a sinusoidal output signal, whereby the simulation time serves as a time base. With a randomly chosen value for the amplitude, the noise signal shown in Fig. 12.
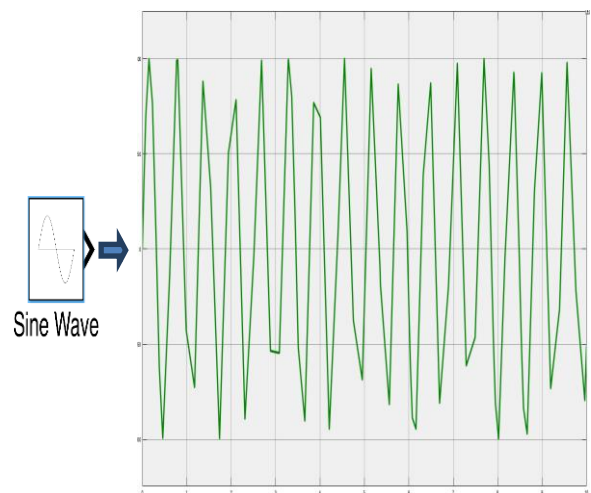

Figure 12: Sine wave interference signal

The interference signal $z(t)$ thus generated has the following effects on the vertical dynamics of the object:

$$\ddot{y}_R(t) = \frac{mg - F_R(t) - k_{Ly}\dot{y}_m(t) + z(t)}{m} \quad \text{and} \tag{73}$$

$$\ddot{y}_m(t) = \frac{mg - F_H(t) - k_{Ly}\dot{y}_m(t) + z(t)}{m}.$$

Due to the prior adjustment of the sliding mode control, there was no change in the function shown in Fig. 11. Setting the parameters λ, $B = 1$ confirms the influence of the disturbance variable on the dynamics (Fig. 13).
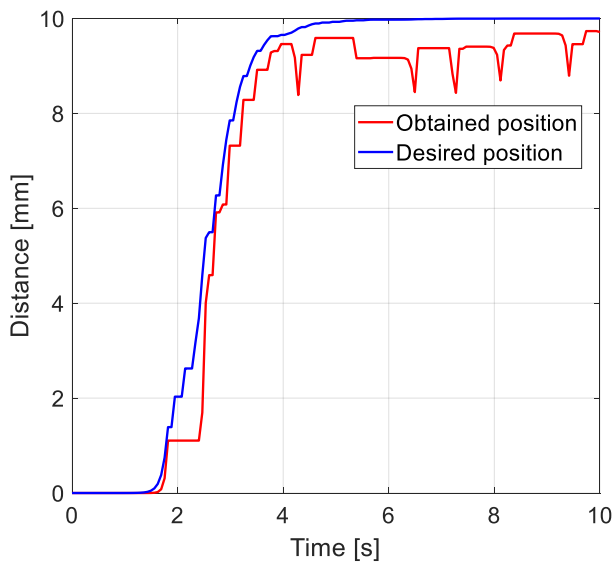

Figure 13: Simulation with a sine interference signal, λ = 1, $B = 1$

Of interest are the limits of λ and B, where the control has instability. A constant parameter $B = 100$ and the simultaneous reduction of λ resulted in no decrease in performance up to a value of λ=389, from which value of an instability resulted, Fig. 14.

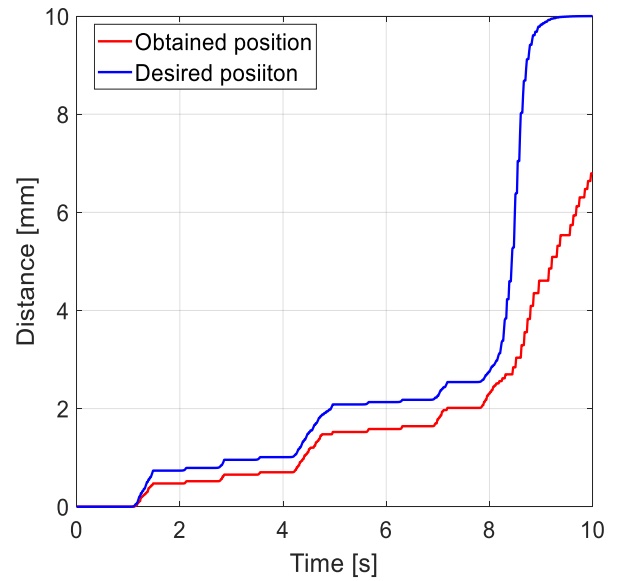Figure 14: Simulation with a sine interference signal, λ = 389, $B = 100$

Keeping the parameter λ = 500 constant and reducing B at the same time did not lead to any change in performance up to a value of $B > 3$; from this value an instability resulted, Fig. 15. With correct dimensioning of the parameters λ and B, the SMC accordingly has a resistance to interference. The rate of change of the switching function thus ensures fulfilment of the stability condition.
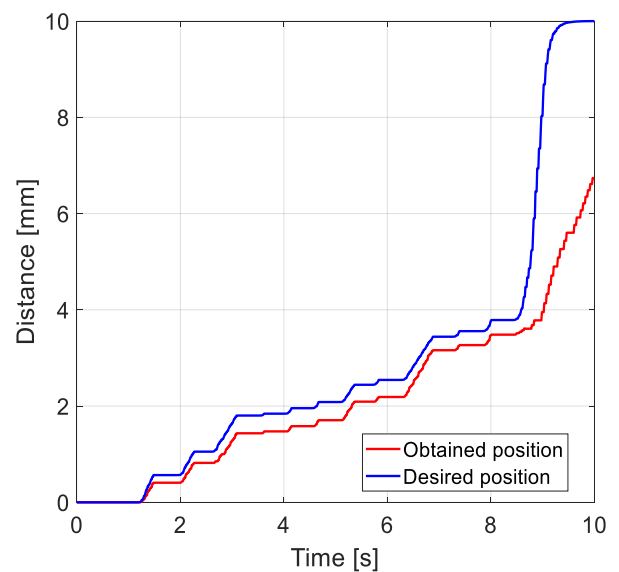

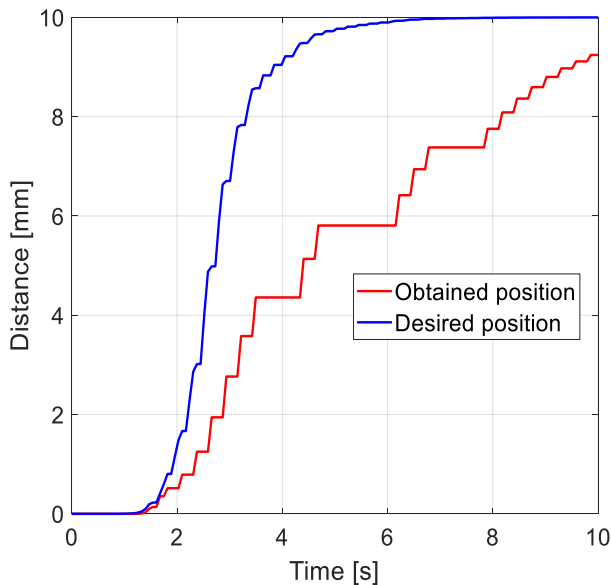Figure 15: Simulation with a sine interference signal, λ = 500, $B = 3$

Figure 16: Simulation with a sine interference signal, $\lambda =$ 100, $B = 1$

Figures 16 and 17 show how, increasing parameter B, maintaining $\lambda = 100$, the performance of the tracking can be improved.
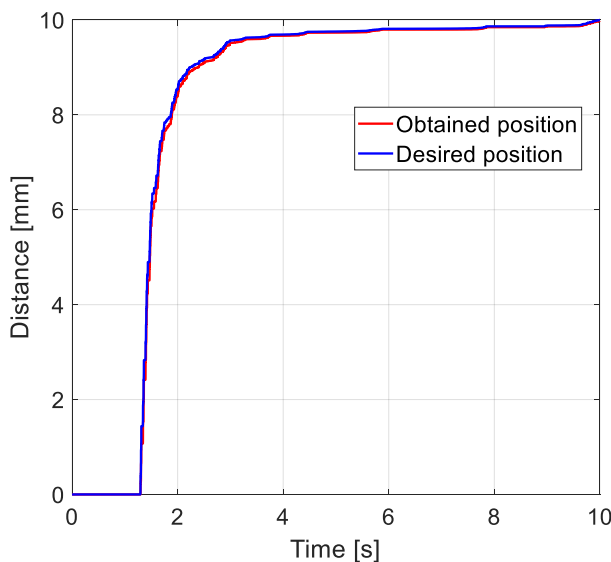

Figure 17: Simulation with a sine interference signal, $\lambda =$ 100, $B = 1000$

6.   Discussion   and   Conclusion

In this work, the vertical position control of an object, using a SMC, has been investigated. First of all, the physical laws concerning the system were explained. In particular, the friction law according to Charles Augustin de Coulomb should be emphasized, as this ensures a nonlinearity within the dynamics. The second step was to describe the dynamic relationships of the system using differential equations. These equations were then transformed into Simulink function blocks to allow simulation of system behaviour. Subsequently, the choice of the Sliding Mode regulation was justified. Proof of whether the use of this regulatory variant has legitimacy was based on the stability theory of Alexander M. Lyapunov. In the analysis of the regulation, the reachability condition of the switching hyperplane was met by matching the veining rate. Furthermore, this parameterization ensured the required uniform motion sequence. The aspect of the research question as to whether a vertical position control can be regulated by specifying the target position has been confirmed by the simulation and analysis. It should be noted that this also has to be considered in the context of simplification. The presence of the nonlinear Coulomb friction was compensated by the Sliding Mode Control. However, not only the factor of nonlinearity, but also the robustness and stability of the control has been proven experimentally. This was done by using a limited random disturbance. To what degree the control is possible to be determined on the basis of this modelling only for the two-dimensional Cartesian coordinate system defined here. According to the analysis, the control is not possible if the parameters of the switching function are defined incorrectly or an unlimited disturbance occurs.

7 Outlook

The simulation has thus shown that this type of position control in the two-dimensional Cartesian coordinate system is possible. Of further interest is now the extension of this system to a three-dimensional space. This analysis is an important preliminary stage to enable the interaction of two robots using this method. By using two cooperating robots, objects could be transported to any position within their environment by combining both contact forces. Since the shape, material type and start position of the object are known in industrial production, it would be possible to define the object centre as the origin of a coordinate system. This would result in the robots being able to orient their centre of effect around the newly created origin of coordinates. When moving in three-dimensional space, rotational movements of the robots play an

essential role. But not only the rotation of the robot axes has to be considered, but also the rotation movement of the object has to be included in the control. Since the findings of this work were derived purely from a simulation, it goes without saying that the practical implementation of these findings is of great interest. This outlook shows that there is a broad spectrum for further theoretical and experimental research based on this approach.

References:

[1] Ferch Tobias, Mercorelli Paolo *Sliding Mode Control for a Vertical Dynamics in the Presence of Nonlinear Friction*, WSEAS Transactions on Circuits and Systems, Volume 18, pp. 102-112, 2019.
[2] Mercorelli Paolo *A robust cascade sliding mode control for a hybrid piezo-hydraulic actuator in camless internal combustion engines*, In IFAC Proc. Volume 45, Issue 13, pp. 790-795, 2012.
[3] Zwerger Tanja, Mercorelli Paolo *Combining an Internal SMC with an External MTPA Control Loop for an Interior PMSM*. In Proc. of the 2018 23rd Int. Conf. on Methods and Models in Automation and Robotics, MMAR 2018, 2018, pp. 674-679
[4] Mercorelli Paolo *An antisaturating adaptive preaction and a slide surface to achieve soft landing control for electromagnetic actuators. In* IEEE/ASME Trans. on Mechatronics, vol.17, n.1, pp.76-85, 2012.
[5] Rust, Wilhelm, *Non-linear finite element analysis in structural mechanics*, Springer, 2015
[6] Garofalo, Franco, Glielmo, Luigi*, Robust Control via Variable Structure and Lyapunov Techniques*, Springer, 1996
[7] Shtessel, Yuri et. al., *Introduction: Intuitive Theory of Sliding Mode Control,* Springer, 2014.
[8] Shtessel, Yuri, *Sliding Mode Control and Observation,*2014.
[9] Slotine, Jean-Jacques E./Li, Weiping, *Applied nonlinear control,* Prentice Hall, 1991
[10] Zinober, Alan S. I., *Variable Structure and Lyapunov Control,* Springer, 1994